

# Superconductivity at 35 K in Graphite-Sulfur Composites

R. Ricardo da Silva\*, J. H. S. Torres, and Y. Kopelevich

*Instituto de Física “Gleb Wataghin”, Universidade Estadual de  
Campinas, Unicamp 13083-970, Campinas, São Paulo, Brasil*

## Abstract

We report magnetization measurements performed on graphite-sulfur composites which demonstrate a clear superconducting behavior below the critical temperature  $T_{c0} = 35$  K. The Meissner-Ochsenfeld effect, screening supercurrents, and magnetization hysteresis loops characteristic of type-II superconductors were measured. It is also found that superconducting correlations persist at temperatures well above  $T_{c0}$ .

74.10.+v, 74.80.-g

A considerable scientific interest to graphite and graphite-based superconducting compounds [1-5] has been renewed [6-8] by the discovery of superconductivity at 39 K in MgB<sub>2</sub> [9], a material similar to graphite both electronically and crystallographically. Besides, recent experiments [10-12] suggested the occurrence of superconducting correlations in highly oriented pyrolytic graphite (HOPG) samples. It has been proposed [13] that a topological disorder in graphene sheets can trigger the superconducting instabilities.

In the present paper we report an unambiguous evidence for the superconductivity occurrence in graphite-sulfur (C-S) composite samples. A clear superconducting behavior is found below the critical temperature  $T_{c0} = 35$  K. Besides, our results demonstrate that the pairing remains significant on a local scale for  $T \gg T_{c0}$ .

The C-S composites were prepared by mixture of the graphite powder consisting of  $\sim 8 \mu\text{m}$  size particles [the impurity content in ppm: Fe (32), Mo (< 1), Cr (1.1), Cu (1.5)] and the sulfur powder (99.998 %; Aldrich Chemical Company, Inc.) in a ratio C:S = 1:1. The mixture was pressed into pellets, held under Ar atmosphere at 650 K for one hour and subsequently annealed at 400 K for 10 hours before cooling to room temperature. The final sulfur contents in the composite was 23 wt %. Dc magnetization and low-frequency ( $\nu = 1$  Hz) standard four-probe resistance measurements were performed on the sample of size  $4.86 \times 4.52 \times 3.52 \text{ mm}^3$  by means of SQUID magnetometer MPMS5 and PPMS commercial equipment (Quantum Design).

X-ray ( $\theta - 2\theta$  geometry) analysis revealed a small decrease in the c-axis lattice parameter of the hexagonal graphite from  $c = 6.721 \text{ \AA}$  in the pristine graphite powder to  $c = 6.709 \text{ \AA}$  in the composite sample, and no changes in the lattice parameters of the orthorhombic sulfur ( $a = 10.45 \text{ \AA}$ ,  $b = 12.84 \text{ \AA}$ ,  $c = 24.46 \text{ \AA}$ ). Figure 1 shows x-ray diffraction pattern of C - 23 wt % S composite obtained with Cu K $\alpha$  source and  $2\theta$  step of  $0.05^\circ$ . As Fig. 1 illustrates, no impurity or additional phases were found.

Figure 2 presents temperature dependencies of the magnetization  $M(T,H) = m(T,H)/V$  ( $m$  is the sample magnetic moment and  $V$  is the sample volume) measured in as-received sample (labeled here as A) at applied fields  $H = 10$  Oe and  $H = 100$  Oe. The magnetization

data corresponding to the zero-field-cooled (ZFC) regime,  $M_{ZFC}(T)$ , were taken on heating after the sample cooling at zero applied field, and the magnetization in the field-cooled on cooling (FCC) regime,  $M_{FCC}(T)$ , was measured as a function of decreasing temperature in the applied field. Figure 2 demonstrates a pronounced difference between  $M_{ZFC}(T)$  and  $M_{FCC}(T)$  which occurs with the temperature decreasing. The inset in Fig. 2 gives a detailed view of the data obtained for  $H = 100$  Oe in a vicinity of the  $T_c(H = 100$  Oe) = 33 K below which a departure of  $M_{ZFC}(T)$  from  $M_{FCC}(T)$  takes place. As can be seen from this plot, both  $M_{ZFC}(T)$  and  $M_{FCC}(T)$  become more diamagnetic at  $T < T_c(H)$ . Such magnetization behavior is characteristic of superconductors: The enhancement of the diamagnetism below the superconducting transition temperature  $T_c(H)$  originates from the screening supercurrents (ZFC regime) and the Meissner-Ochsenfeld effect of magnetic flux expulsion (FCC regime). It can also be seen in Fig. 2 that as the applied field increases, the normal state orbital diamagnetism of graphite overcomes a positive contribution to the magnetization (which can be due to both intrinsic weak ferromagnetism of graphite [11, 13, 14] and magnetic impurities) resulting in a negative total magnetization above  $T_c$ .

Figure 3 depicts the normalized ZFC magnetization  $M(T)/|M(50K)|$  measured for various applied fields demonstrating that the transition temperature  $T_c(H)$  decreases with the field increasing as well as that the  $H = 10$  kOe completely suppresses the superconducting response. The obtained  $T_c(H)$  is given in the magnetic field – temperature (H-T) plane, Fig. 4.

Figure 5 (a) presents a magnetization hysteresis loop  $M(H)$  measured at  $T = 6$  K after cooling the sample from 300 K to the target temperature in a zero applied field. In Fig. 5 (b) we show the same data after subtraction of diamagnetic background signal. Figure 5 (a, b) provides an unambiguous evidence that our sample is type-II superconductor with a strong vortex pinning [15, 16].

In contrast to alkali-metal-doped graphite samples in which the superconductivity vanishes after a short-time sample annealing at  $T \geq 100$  K [3], the superconducting properties in our sample were stable during one week of measurements in the temperature range 5

$K \leq T \leq 300$  K. To verify further the superconductivity stability, the sample was kept at ambient conditions for two weeks. During this time the sample has lost about 4 wt % of sulfur. Then, we found a small decrease in  $T_c(H)$  and a strong reduction in magnitude of the superconducting response. The inset in Fig. 4 exemplifies  $M_{ZFC}(T)$  and  $M_{FCC}(T)$  recorded for this sample (labeled here as B) in applied field  $H = 100$  Oe. The transition temperature  $T_c(H)$  measured in the sample B for several  $H$  is shown in Fig. 4. Figure 6 (a) presents  $M(H)$  hysteresis loop obtained at  $T = 6$  K. Notably, the superconducting hysteresis loops could also be resolved at  $T \gg T_c$ . Figure 6 (b) illustrates this fact where  $M(H)$  obtained at  $T = 100$  K is shown. In other words, this observation suggests that pairing remains significant well above  $T_c$ . While the high-temperature  $M$  vs.  $H$  measurements were not performed on the sample A, one can anticipate that the superconductivity persists above  $T_c$  in the sample A as well.

We proceed with a discussion of the results noting that the zero-field resistance  $R(T)$  measurements (not shown here) performed on the sample A revealed a slight increase ( $\sim 20$  %) of the resistance lowering temperature from 300 K to  $T_{on} \approx 35$  K, and its rapid growth with a further temperature decrease,  $T \leq T_{on}$ . The measured  $R(T)$  resembles the resistance behavior in ultrathin films consisting of isolated superconducting “islands” where  $T_{on}$  coincides with  $T_c$  of the bulk material [17]. Actually, a small magnitude of the Meissner signal, see Fig. 2, can result from a small size  $L < \lambda$  ( $\lambda$  is the penetration depth) of the “islands”.

It is tempting to relate  $H(T_c)$ , Fig. 4, to the upper critical field boundary. However, a different interpretation of  $H(T_c)$  is also possible. It is found that  $H(T_c)$  can be best described by the power law:

$$H = H^*(1 - T_c/T_{c0})^{3/2} \quad (1)$$

in a vicinity of  $T_{c0} = 35$  K, and by the equation:

$$H = H_0 \exp(-T_c/T_0) \quad (2)$$

below a reduced temperature  $T/T_{c0} \sim 0.8$ , where  $H_0 = 5$  T and  $T_0 = 7$  K, see Fig. 4. Equations (1) and (2) imply that  $H(T_c)$  can be accounted for by the existence of a breakdown field  $H_b(T)$  which destroys the superconductivity induced by a proximity effect [18-20]. According to the theory [20],  $H_b(T)$  for normal-metal-superconductor (NS) structures saturates in the limit  $T \rightarrow 0$  to a value  $H_b(T = 0) \approx 0.37H_0$ . Taking  $H_0 = 5$  T, one gets  $H_b(T = 0) = 1.85$  T which agrees well with the experimentally determined field  $H = 1$  T at which the superconducting response vanishes, see Fig. 3.

We note further that  $T_c(H)$  measured in samples A and B differs by a few Kelvin only (Fig. 3), whereas the superconducting shielding effect as well as the magnetization hysteresis width are strongly suppressed in the sample B. These results can be understood assuming that a size of superconducting “islands” in the sample B is much smaller than that in the sample A ( $L_B \ll L_A$ ).

Finally, we stress that no sign of the superconductivity was found in our pristine graphite powder. On the other hand, the highest  $T_c = 17$  K in sulfur was reached under pressure of 160 GPa [22]. We speculate that the superconductivity in C-S composites originates from a sulfur-carbon interaction at the graphite surface. Similar to the effect of adsorbed gases [23, 24], a hybridization between carbon and sulfur can increase the local charge density and therefore trigger the superconductivity. Further studies should verify this hypothesis.

To conclude, the above results provide an unambiguous evidence for the occurrence of high-temperature superconductivity in graphite-sulfur composite samples and open new perspectives for the engineering of graphite-based superconductors with high  $T_c$ .

This work was supported by FAPESP, CNPq, and CAPES Brazilian science agencies.

## REFERENCES

(\*) Also at FAENQUIL, 12600-000, Lorena, SP, Brasil

[1] N. B. Hannay, T. H. Geballe, B. T. Matthias, K. Andres, P. Schmidt, and D. MacNair, Phys. Rev. Lett. 14, 225 (1965).

[2] Y. Koike, S.-I. Tanuma, H. Suematsu, and K. Higuchi, J. Phys. Chem. Solids 41, 1111 (1980).

[3] I. T. Belash, A. D. Bronnikov, O. V. Zharikov, and A. V. Palnichenko, Solid State Commun. 64, 1445 (1987); ibid. 69, 921 (1989).

[4] A. Chaiken, M. S. Dresselhaus, T. P. Orlando, G. Dresselhaus, P. M. Tedrow, D. A. Neumann, and W. A. Kamitakahara, Phys. Rev. B 41, 71 (1990).

[5] R. A. Jishi and M. S. Dresselhaus, Phys. Rev. B 45, 12465 (1992).

[6] K. D. Belashchenko, M. van Schilfgaarde, and A. P. Antropov, cond-mat/0102290.

[7] J. M. An and W. E. Pickett, Phys. Rev. Lett. 86, 4370 (2001).

[8] G. Baskaran, cond-mat/0103308.

[9] J. Nagamatsu, N. Nakagawa, T. Muranaka, Y. Zenitani, and J. Akimitsu, Nature 410, 63 (2001).

[10] Y. Kopelevich, V. V. Lemanov, S. Moehlecke, and J. H. S. Torres, Fizika Tverd. Tela (St. Petersburg) 41, 2135 (1999) [Phys. Solid State 41, 1959 (1999)].

[11] Y. Kopelevich, P. Esquinazi, J. H. S. Torres, and S. Moehlecke, J. Low Temp. Phys. 119, 691 (2000).

[12] H. Kempa, Y. Kopelevich, F. Mrowka, A. Setzer, J. H. S. Torres, R. Höhne, and P. Esquinazi, Solid State Commun. 115, 539 (2000).

[13] J. Gonzales, F. Guinea, and M. A. H. Vozmediano, Phys. Rev. B 63, 13442 (2001).

[14] D. V. Khveshchenko, cond-mat/0101306.

[15] Y. B. Kim, C. F. Hempstead, and A. R. Strnad, Phys. Rev. 129, 528 (1963).

[16] Y. Yeshurun, A. P. Malozemoff, and A. Shaulov, Rev. Mod. Phys. 68, 911 (1996).

[17] B. G. Orr, H. M. Jaeger, and A. M. Goldman, Phys. Rev. B 32, 7586 (1985).

[18] G. Deutscher and P. G. de Gennes, in *Superconductivity*, edited by R. Parks (Marcel Dekker, New York, 1969), Vol. 2.

[19] G. Deutscher and A. Kapitulnik, *Physica A* 168, 338 (1990).

[20] A. L. Fauchère and G. Blatter, *Phys. Rev. B* 56, 14102 (1997).

[21] M. S. Dresselhaus and G. Dresselhaus, *Adv. Phys.* 30, 139 (1981).

[22] V. V. Struzhkin, R. J. Hemley, H.-K. Mao, and Y. A. Timofeev, *Nature* 390, 382 (1997).

[23] S. M. Lee, Y. H. Lee, Y. G. Hwang, J. R. Hahn, and H. Kang, *Phys. Rev. Lett.* 82, 217 (1999).

[24] P. Ruffieux, O. Gröning, P. Schwaller, L. Schlapbach, and P. Gröning, *Phys. Rev. Lett.* 84, 4910 (2000).

## FIGURES

Fig. 1. X-ray  $\theta$ - $2\theta$  diffraction pattern of the C - 23 wt % S composite.

Fig. 2. Temperature dependencies of the magnetization  $M(T)$  measured in as-received sample (A) in zero-field-cooled (ZFC) and field-cooled on cooling (FCC) regimes at two applied fields; 10 Oe and 100 Oe. Inset gives enlarged view of the superconducting transition recorded at  $H = 100$  Oe.

Fig. 3. Normalized ZFC magnetization measured in sample A at various applied fields. Arrows denote the superconducting transition temperature  $T_c(H)$ .

Fig. 4.  $H(T_c)$  for samples A and B. Dashed and dotted lines are obtained from Eq. (1) and Eq. (2) with the fitting parameters  $T_{c0} = 35$  K,  $H^* = 0.9$  T,  $T_0 = 7$  K, and  $H_0 = 5$  T. Inset presents  $M(T)$  measured in sample B at  $H = 100$  Oe.

Fig. 5. (a) Magnetization hysteresis loop  $M(H)$  measured in the sample A at  $T = 6$  K; (b)  $M(H)$  obtained after subtraction of the diamagnetic background signal  $M = -\chi H$  with  $\chi = 3.5 \times 10^{-3}$  mG/Oe.

Fig. 6. Magnetization hysteresis loops obtained for the sample B at  $T = 6$  K (a) and  $T = 100$  K (b) after subtraction of the diamagnetic background signal  $M = -\chi H$  with  $\chi = 3.5 \times 10^{-3}$  mG/Oe (6 K) and  $\chi = 3.3 \times 10^{-3}$  mG/Oe (100 K).

Fig. 1

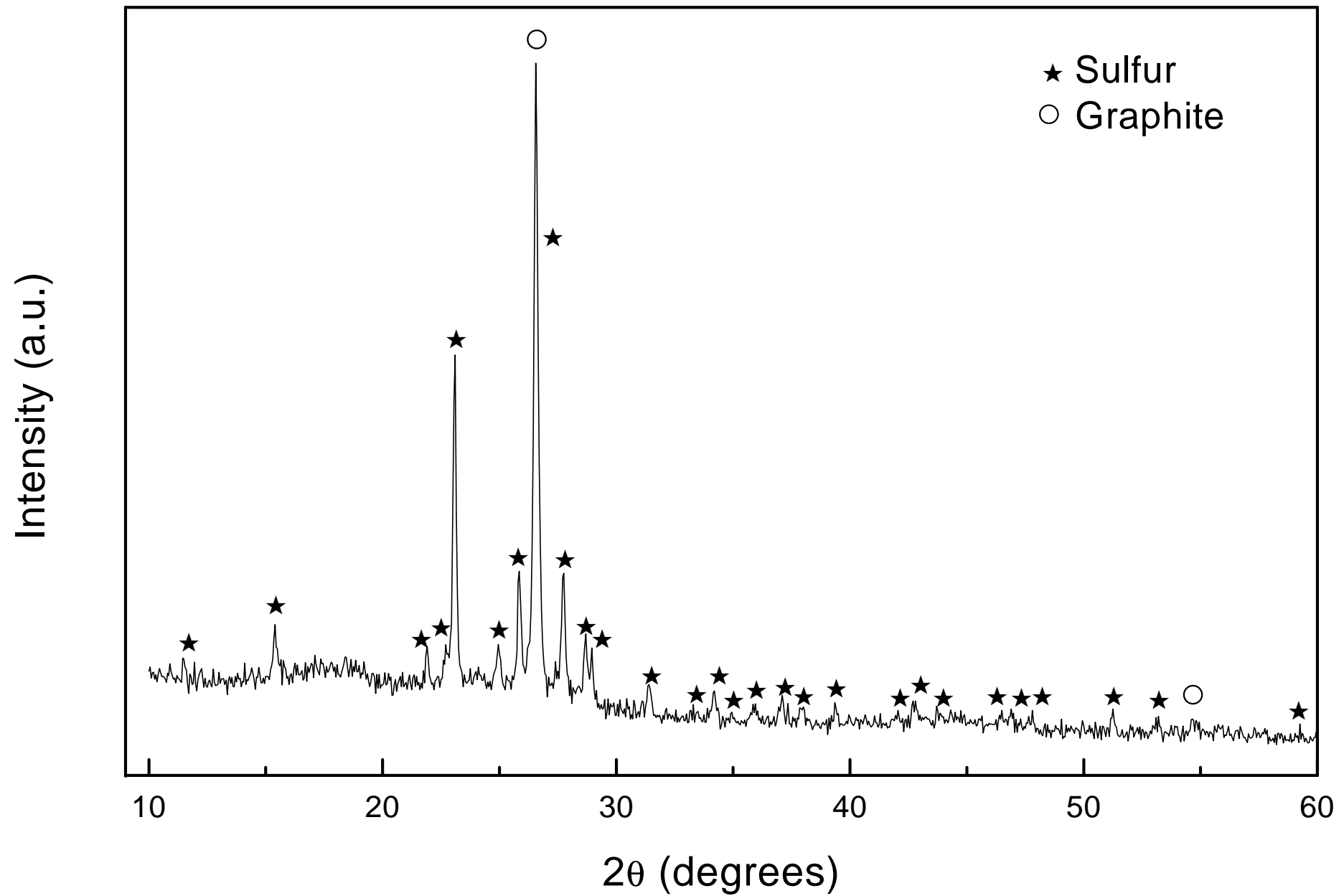


Fig. 2

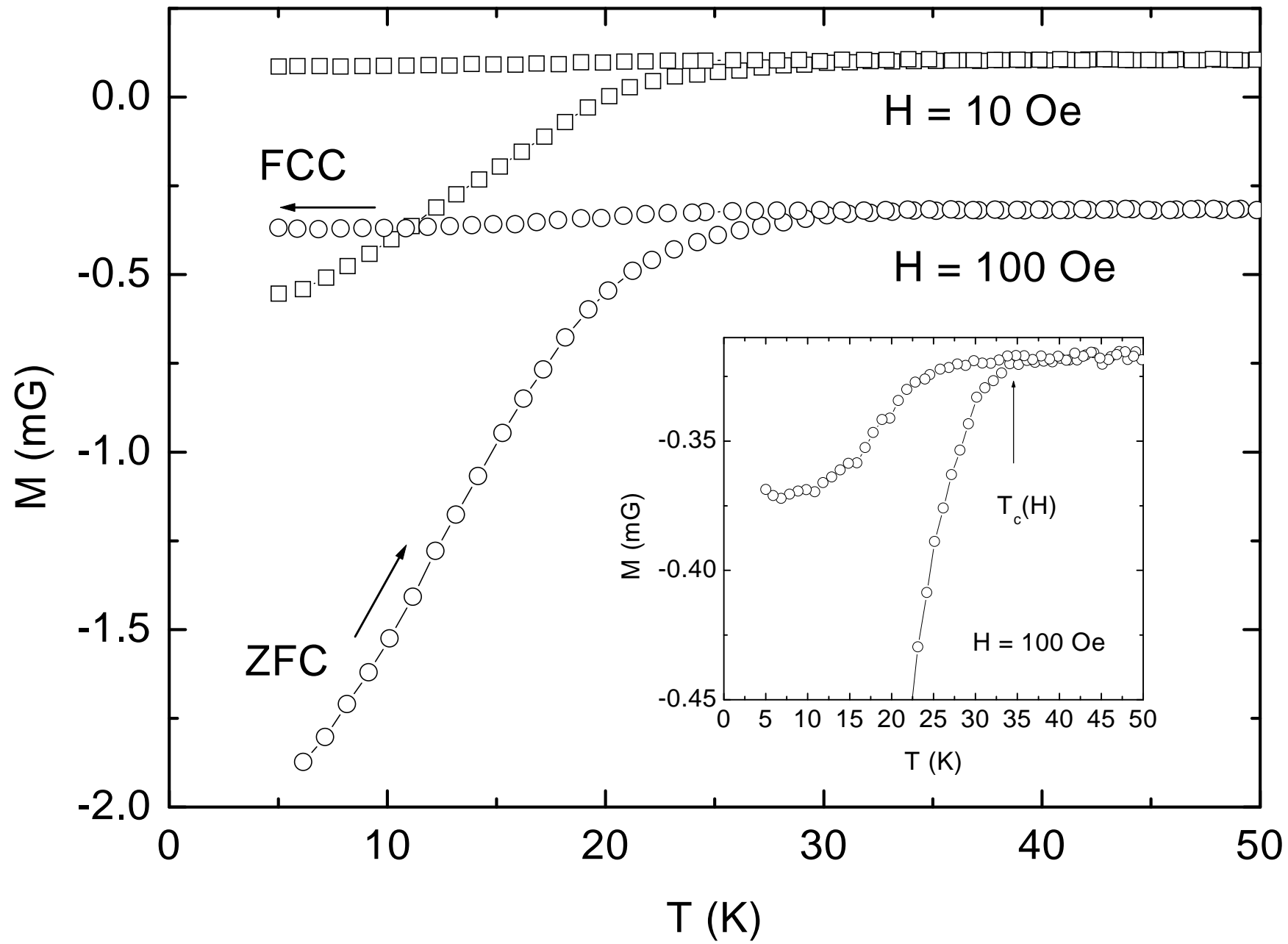


Fig. 3

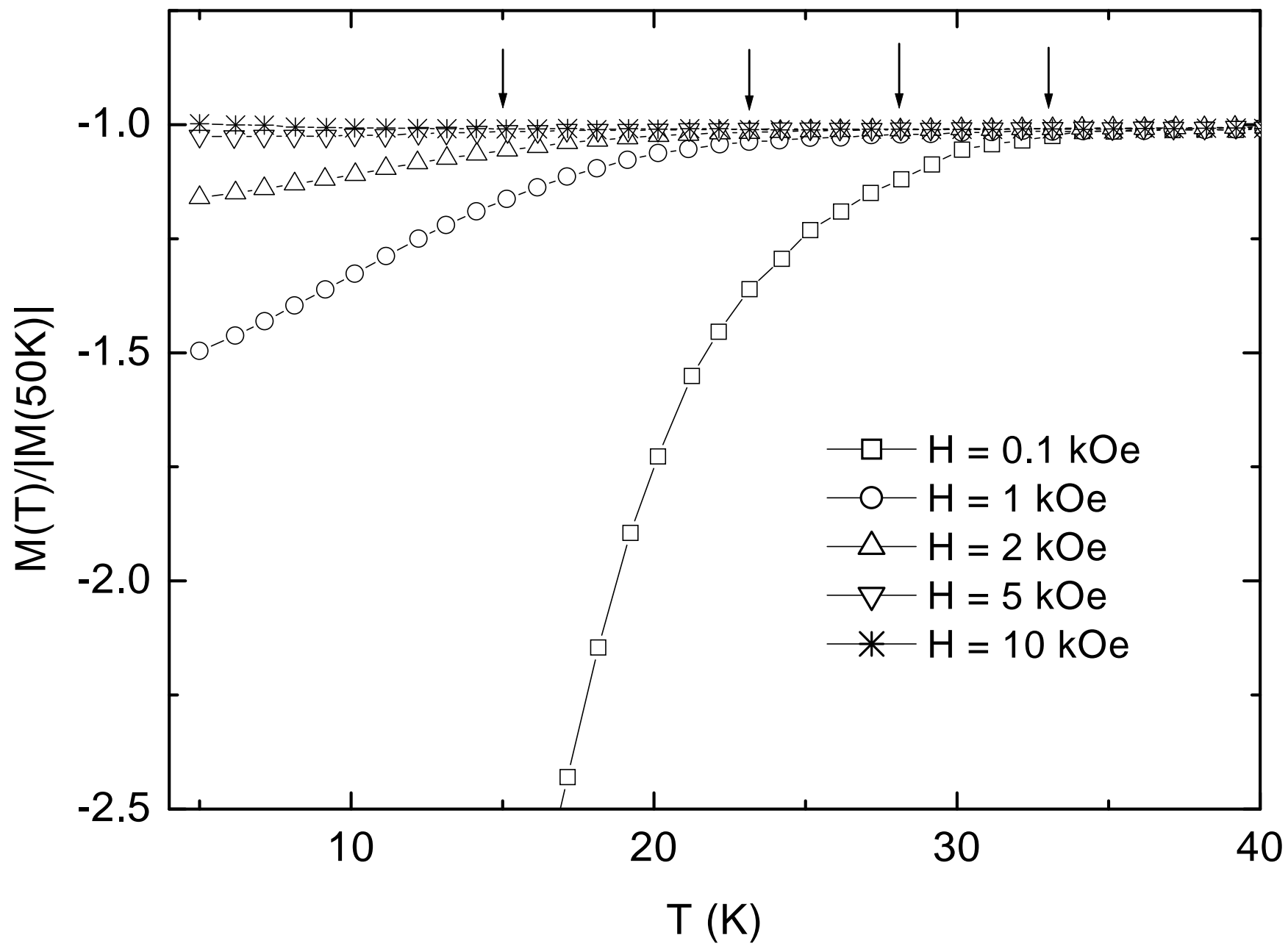


Fig. 4

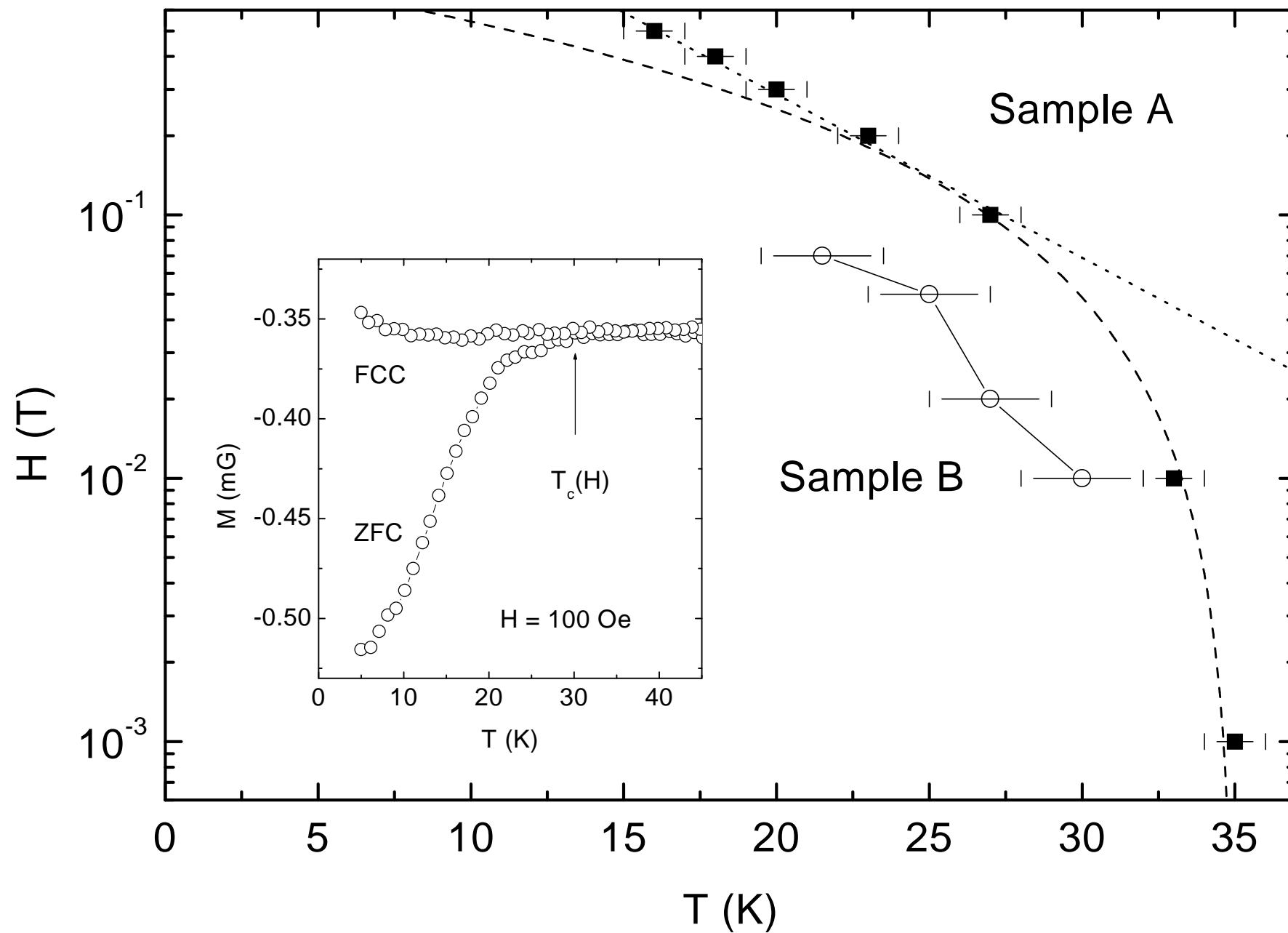


Fig. 5

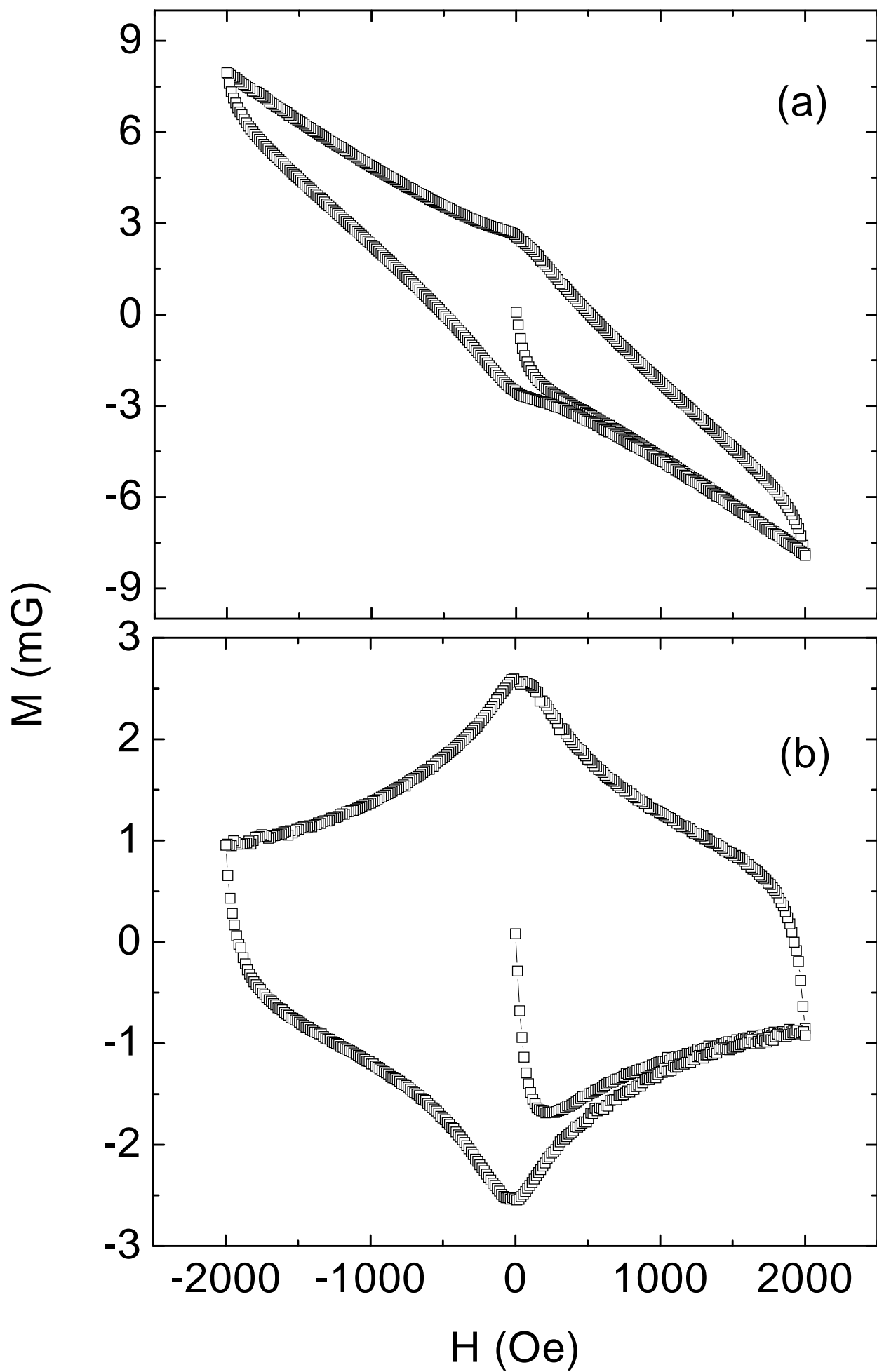


Fig. 6

